International Journal of Nanomedicine

Dovepress
open access to scientific and medical research

Open Access Full Text Article

ORIGINAL RESEARCH

Nanomicelles loaded with doxorubicin and curcumin for alleviating multidrug resistance in lung cancer

This article was published in the following Dove Press journal:
International Journal of Nanomedicine
3 November 2016
Number of times this article has been viewed

Yue Gu[1,*]
Jing Li[2,*]
Yang Li[1]
Lei Song[1]
Dan Li[1]
Liping Peng[1]
Ying Wan[3]
Shucheng Hua[1]

[1]Department of Respiratory and Critical Care Medicine, the First Affiliated Hospital of Jilin University, Changchun, Jilin, [2]Hubei Province Key Laboratory on Cardiovascular, Cerebrovascular, and Metabolic Disorders, Hubei University of Science and Technology, Xianning, [3]College of Life Sciences and Technology, Huazhong University of Science and Technology, Wuhan, Hubei, People's Republic of China

*These authors contributed equally to this work

Purpose: A new type of polymeric micelle (PM) was assembled using a polyethylene glycol (PEG)-linked (PEGylated) amphiphilic copolymer and D-tocopheryl PEG_{1000} succinate ($TPGS_{1000}$). The micelles were used to deliver doxorubicin (DOX) and curcumin (CUR) for alleviating multidrug resistance (MDR) in lung cancer cells while enhancing the therapeutic efficacy of DOX.

Methods: Micelles loaded with DOX and CUR were assembled using a film-forming technique. Micelles were used to treat A549/Adr cells to find out whether micelles had the ability to reverse the MDR of A549/Adr cells. Some investigations were conducted using tumor-bearing mice to assess whether these micelles had enhanced antitumor efficacy as compared to DOX alone or the combination of DOX and CUR.

Results: Some micelles (DOX + CUR)–PMs had a small average size of about 17 nm and showed definite ability to deliver both DOX and CUR into DOX-resistant A549/Adr cells. The PMs had high cytotoxicity toward A549/Adr cells when the applied equivalent DOX dose was 1 μg/mL or higher. The cellular uptake of (DOX + CUR)–PMs into A549/Adr cells was found to be associated with an energy-dependent, caveolae-mediated, and clathrin-independent mechanism. (DOX + CUR)–PMs helped to prolong the circulation of DOX or CUR as compared to the individual administration of DOX or CUR, and they exhibited high inhibiting efficiency against the growth of tumors and were able to reduce the side effects of DOX.

Conclusion: $TPGS_{1000}$ and CUR could synergistically reverse DOX-resistance of A549/Adr cells. In vivo examinations confirmed that the micelles had the capability to increase the plasma concentration of DOX or CUR, as well as to prolong their respective blood circulation. These micelles were able to significantly inhibit tumor growth in Lewis lung carcinoma tumor-bearing mice while reducing the side effects of DOX. The micelles showed potential in the treatment of lung cancer.

Keywords: synergistic effect, drug-resistance, doxorubicin, curcumin, polymeric micelles

Introduction

The resistance of human tumors to multiple chemotherapeutic agents, commonly called as multidrug resistance (MDR), has been recognized as a major obstacle in the effective treatment of many malignancies.[1] MDR can occur mainly due to two reasons: 1) tumor cells may be inherently resistant to certain chemotherapeutic agents due to their genetic characteristics; and 2) tumor cells could acquire resistance after being constantly exposed to a chemotherapeutic drug for a long period of time. The second one is the main cause of the failure of chemotherapy.[1,2] To enhance the therapeutic efficacy of chemotherapeutic agents involved in MDR-related cancer therapies,

Correspondence: Ying Wan
College of Life Sciences and Technology, Huazhong University of Science and Technology, Wuhan, Hubei 430074, People's Republic of China
Tel +86 27 8779 2147
Fax +86 27 8779 2234
Email ying_wan@hust.edu.cn

Shucheng Hua
Department of Respiratory and Critical Care Medicine, the First Affiliated Hospital of Jilin University, Changchun, Jilin 130021, People's Republic of China
Tel +86 431 8565 4528
Fax +86 431 8878 2442
Email shuchenghua@aliyun.com

the issue of how to overcome MDR of cancer cells often needs to be addressed regardless of the cause.[1–3]

Doxorubicin (DOX) is an anthracycline glycoside antibiotic and has a broad spectrum of antitumor activity against a variety of solid tumors, including cancers of the breast, endometrium, liver, bile duct, esophagus, and bone.[4–7] Despite its wide use in the clinic, DOX can result in severe side effects, mainly including cardiotoxicity, bone marrow suppression, as well as hematological and testicular toxicity.[8] In addition, a range of tumors has developed resistance to this drug.[8,9] A few synthetic small molecules and antibodies, which show various abilities to inhibit the actions of MDR-related proteins, have been used to improve therapeutic efficacy of DOX but their functions are limited because of their undesirable effects and low stability.[8] In recent years, several natural herbs have aroused increasing interest in cancer chemotherapy due to their sensitization functions.[10–12] Different natural herbs have already been used together with different chemotherapeutic agents, and enhanced efficacies along with reduced side effects for these chemotherapeutic agents have been reported.[13,14]

Among the optional herbs, curcumin (CUR) has been extensively investigated because it can induce apoptosis – or even death – of the sensitized cancer cells by inhibiting the activity of human epidermal growth factor receptor-2 and nuclear factor κB.[15,16] CUR is also an effective sensitizer that can restrict the activity of some MDR-related proteins and inhibit different types of cancer cells from proliferating.[17,18] Therefore, it will be feasible to use DOX and CUR together for alleviating MDR of some cancer cells while enhancing the therapeutic efficacy of DOX. Nevertheless, a simple blend of DOX and CUR will not be a favorable formulation for their combined use because CUR has poor aqueous solubility and low bioavailability; moreover, CUR could be rapidly cleared by the circulation.[19,20]

To date, several nanocarriers involving liposomes, polyethylene glycol (PEG)-linked (PEGylated) polycaprolactone nanoparticles and chitosan/poly(butyl cyanoacrylate) nanoparticles have been used to deliver DOX and CUR together.[21–24] Although these nanocarriers have shown improved anticancer efficacy against different tumors, whether they have the potential to reverse MDR of cancer cells has not been examined. In this study, an attempt has been made to develop a new type of nanocarrier that can deliver DOX together with CUR to inhibit the growth of certain lung cancer cells showing MDR characteristics. To achieve this, a type of (DOX + CUR)-loaded polymeric micelle (PM) was assembled using 1,2-distearoyl-*sn*-glycero-3-phosphoethanolamine-*N*-methoxy-poly(ethylene glycol)$_{2000}$ (DSPE-PEG$_{2000}$) and D-tocopheryl polyethyleneglycol$_{1000}$ succinate (TPGS$_{1000}$). Of these selected materials, DSPE-PEG$_{2000}$ is a biodegradable amphiphilic copolymer with self-assembly features.[25,26] The DSPE-PEG$_{2000}$ component in PMs contributes to the construction of a hydrophobic core for loading both DOX and CUR and, at the same time, to the formation of a hydrophilic shell for favorable in vivo circulation. Another component in PMs, namely, TPGS$_{1000}$, is one of the membrane efflux transporters and has inhibiting functions against the adenosine triphosphate (ATP)-dependent pump P-glycoprotein (P-gp).[27–29] In addition to its application in enhanced chemotherapy, TPGS has recently been used as a component to modify solid–lipid nanoparticles for overcoming P-gp-mediated MDR related to leukemia.[30] In these applications, TPGS$_{1000}$ has shown certain ability to inhibit the exocytosis of the internalized nanoparticles from cancer cells.[27–30] Therefore, it would be possible to help DOX to circumvent the MDR-associated pathways in some cancer cells while enhancing the anticancer efficacy of DOX if the carriers used for the delivery of DOX could be built using DSPE-PEG$_{2000}$ and TPGS$_{1000}$.

Although some vehicles for the co-delivery of DOX and CUR have been investigated,[21–24] nanocarriers that have an ability to overcome MDR of certain lung cancer cells, in addition to being able to enhance the therapeutic efficacy of DOX against lung cancer, are still few. Some (DOX + CUR)-loaded PMs have been thus assembled using a film-forming technique, and the assembling conditions have been optimized to achieve desirable ones with small sizes and high drug loadings (DLs). The obtained PMs have been examined to see whether they had the ability to reverse the MDR of certain lung cancer cells. Some in vivo investigations on these PMs have also been conducted using Lewis lung carcinoma (LLC) tumor-bearing C57BL/6 mice to assess their antitumor efficacy.

Materials and methods

Materials

DOX-HCl and DSPE-PEG$_{2000}$ were bought from Norzer (Beijing, China) and NOF Corporation (Tokyo, Japan), respectively. CUR, TPGS$_{1000}$, sulforhodamine B, MTT, and trypsin were purchased from Sigma-Aldrich (St Louis, MO, USA). Dulbecco's minimum essential medium (DMEM), Roswell Park Memorial Institute (RPMI)-1640 medium, and fetal bovine serum (FBS) were obtained from Thermo Fisher Scientific (Waltham, MA, USA). High-performance liquid chromatography (HPLC)-grade solvents were supplied by Sayfo (Tianjin, China). All other reagents and chemicals

were of analytical grade and obtained from Sinopharm, Beijing, China.

Assembly of PMs

DOX-HCl at 2 mg/mL concentration (20 mL) was stirred with twice the number of moles of triethylamine in dimethyl sulfoxide overnight to obtain the DOX free base. After that, CUR (5 mg), $TPGS_{1000}$ (100 mg), and $DSPE\text{-}PEG_{2000}$ (20 mg) were added to a solution of DOX in methanol with stirring for 20 min. The organic solvent was removed using a rotary evaporator under reduced pressure. The drug-loaded film was hydrated at 37°C for 10 min using normal saline. The mixture was centrifuged at 12,000 rpm for 10 min and filtered using 0.22 µm filters to achieve the micelles. The so-produced micelles were referred to as (DOX + CUR)–PMs. A schematic illustration for the assembly of (DOX + CUR)–PMs is presented in Figure 1.

To determine the DL and the loading efficiency (LE) of the PMs, (DOX + CUR)–PMs were dispersed in methanol and subjected to ultrasonic treatment in order to extract DOX and CUR. The content of DOX or CUR in the micelles was analyzed using HPLC (Eclipse XDB-C_{18} column, 150×4.6 mm, 5 µm) under the following running conditions: mobile phase, methanol containing 3 mM monopotassium phosphate, and acetic acid (methanol/monopotassium phosphate/acetic acid/water =230/20/2/748, v/v); flow rate, 1.0 mL/min; injection volume, 20 µL; column temperature, 25°C; and detection wavelength, 227 nm. DL and LE were calculated using the following formulas:

$$DL\ (\%) = (M_0/M) \times 100\% \quad (1)$$

$$LE\ (\%) = (M_0/M_1) \times 100\% \quad (2)$$

where M_0 is the mass of DOX or CUR encapsulated inside micelles and M_1 is the mass of feeding DOX or CUR, with M denoting the mass of micelles.

Characterization

PM suspensions were prepared using ultrapure water and detected using a dynamic light scattering instrument (DAWN® HELEOS™; Wyatt Technology, Santa Barbara, CA, USA) to determine the size distribution and zeta potential of the (DOX + CUR)–PMs. The morphology of (DOX + CUR)–PMs was viewed using transmission electron microscopy (TEM) by putting a drop of suspension onto carbon-coated copper grids and negatively staining with 1% uranyl acetate. The colloidal stability of (DOX + CUR)–PMs was assessed by incubating them with 1% and 10% bovine serum albumin (BSA) at 37°C for 24 h, respectively.

In vitro release

The release profiles of DOX and CUR from the (DOX + CUR)–PMs were determined using a dialysis method. (DOX + CUR)–PMs were introduced into membrane tubes (molecular weight cutoff: 14,000 Da), and the tubes were fully immersed in phosphate-buffered saline (PBS; pH 7.4) containing 0.1% Tween 80. At predetermined time intervals, an aliquot of release medium (1 mL) was withdrawn while replenishing with the same volume of fresh buffer, and the released DOX or CUR was measured using HPLC under the same running conditions mentioned earlier. Three specimens were measured for each sample.

Cytotoxicity analysis

Human lung cancer cells, A549 cells (DOX-sensitive), A549/Adr cells (P-gp overexpressing, DOX-resistant), and

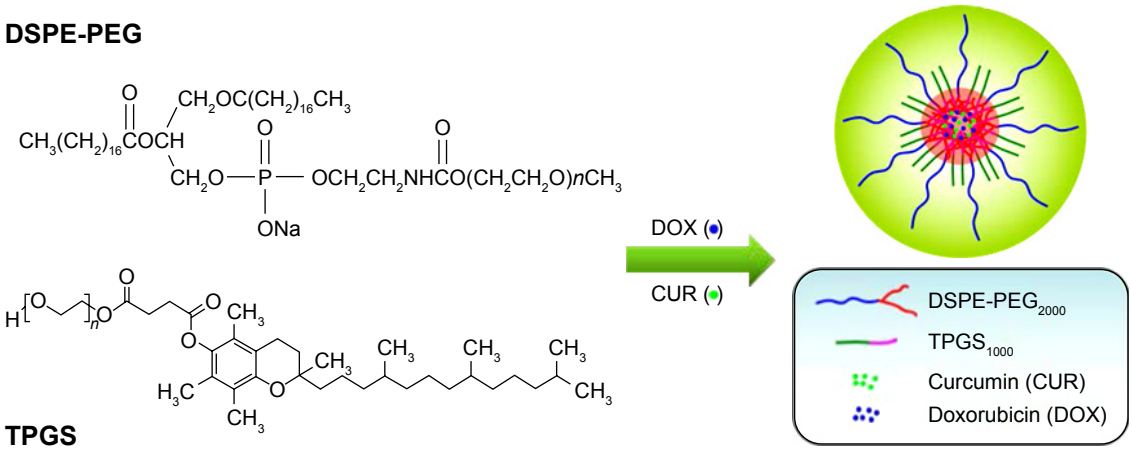

Figure 1 Schematic illustration of (DOX + CUR)–PMs assembled using $DSPE\text{-}PEG_{2000}$ and $TPGS_{1000}$.
Abbreviations: CUR, curcumin; DOX, doxorubicin; $DSPE\text{-}PEG_{2000}$, 1,2-distearoyl-*sn*-glycero-3-phosphorthanolamine-*N*-methoxy-poly(ethylene glycol)$_{2000}$; PMs, polymeric micelles; $TPGS_{1000}$, D-tocopheryl polyethyleneglycol$_{1000}$ succinate.

murine L929 cells were obtained from the Cell Bank of Peking Union Medical University (Beijing, China), and the Cell Bank obtained these cell lines from ATCC (American Type Culture Collection, USA). The present study did not deal directly with patients, medical records, or human tissues, and patient consent was therefore not required. A549 or L929 cells were cultured in DMEM supplemented with 10% FBS and 1% penicillin–streptomycin at 37°C in 5% CO_2 atmosphere. In the case of A549/Adr cells, they were cultured in complete medium containing 1 μg/mL of DOX. In addition, murine LLC cells (Type Culture Collection of the Chinese Academy of Sciences, Beijing, China), which are frequently used in preclinical studies,[31] were cultured in RPMI-1640 supplemented with 10% FBS and 1% penicillin–streptomycin at 37°C in 5% CO_2 humidified atmosphere, and the culture medium was refreshed twice a week until cell confluence. The four types of cells were respectively resuspended in PBS for further use.

To see the impact of blank micelles on the growth of normal cells, L929 cells (96-well plate, 1×10^4 cells per well) were exposed to blank micelles at varied doses changing from 6.25 to 200 μg/mL, and their viability was measured using the MTT assay.

In regard to A549 and A549/Adr cells, they were treated with different DOX-containing agents at various doses to test their viability. Briefly, A549 and A549/Adr cells were respectively seeded in 96-well culture plates at a density of 1×10^4 cells per well and incubated in the complete medium for 24 h. These wells were divided into different groups and respectively exposed to DOX, DOX + CUR, or (DOX + CUR)–PMs at prescribed equivalent DOX doses of 0.05, 0.2, 0.4, 0.6, 0.8, or 1 μg/mL for A549 cells and 1, 2, 5, 10, 20, or 30 μg/mL for A549/Adr cells. The applied amount of CUR was 1.6 times as much as DOX in both cases, respectively corresponding to A549 and A549/Adr cells. These cells were additionally incubated for up to 72 h, and the cell viability was assessed using the MTT assay.

Cellular uptake

To determine the uptake of different agents in A549/Adr cells, the cells were plated in 6-well dishes at a density of 1×10^6 cells per well, and each well was provided with a microscope slide for cell climbing. After 24 h culturing in complete medium, the cells were treated with DOX, CUR, DOX + CUR, and (DOX + CUR)–PMs, respectively. The equivalent DOX dose was 10 μg/mL, while the CUR dose was 16 μg/mL. After 2 h treatment, the cells were washed with cold PBS, fixed with 4% paraformaldehyde for 10 min and stained with 4′,6-diamidino-2-phenylindole to label the cell nucleus. The stained cells were viewed using confocal laser scanning microscopy (CLSM; Olympus, Tokyo, Japan).

Flow cytometry

To figure out the possible mechanism for the uptake of (DOX + CUR)–PMs into A549/Adr cells, A549/Adr cells were respectively treated with different endocytosis inhibitors for a short period of time, and then, the treated A549/Adr cells were exposed to (DOX + CUR)–PMs in combination with one of the used endocytosis inhibitors for an additional culture duration. The internalized amount of (DOX + CUR)–PMs in the A549/Adr cells was measured using a flow cytometer. In brief, A549/Adr cells were seeded in 6-well plates at a density of 5×10^4 cells per well and allowed to attach for 24 h in complete media. All wells were divided into 6 groups with 3 wells in each group. The first 4 groups (Groups 1, 2, 3, and 4) were respectively pretreated with chlorpromazine (10 μg/mL), quercetin (40 μg/mL), indomethacin (100 μg/mL), and β-cyclodextrin (2 mg/mL) for 1 h at 37°C. Afterward, each group was treated with (DOX + CUR)–PMs in conjunction with an endocytosis inhibitor among the 4 mentioned earlier for another 1 h at 37°C, and the applied dose for each type of endocytosis inhibitor was maintained the same as that indicated earlier. Group 5 was used to examine the effect of culture temperature on the endocytosis of (DOX + CUR)–PMs. A549/Adr cells in Group 5 were cultured in complete medium at 4°C for 1 h without pretreatment using endocytosis inhibitor, and they were then exposed to (DOX + CUR)–PMs and cultured at 4°C for another 1 h. The remaining group (Group 6) was used as the control, and this group was processed in the same way as Group 5 but by setting the culture temperature at 37°C. The applied equivalent amount of DOX and CUR for all groups was 10 and 16 μg/mL, respectively.

After completion of the designated incubation, cells in all groups were washed with PBS and treated with trypsin. PBS (1.0 mL) was then added to each well, and the mixture in each well was centrifuged at 5,000 rpm for 5 min. After removal of the supernatants, the collected cell pellets were washed twice with cold PBS, and cell suspensions were subjected to follow-up measurements using a flow cytometer (Coulter FC500, Beckman, Piscataway, NJ, USA). Data for the 10,000 gated events were collected and analyzed following ModFit LT 3.0 program.

Blood clearance

The animal experiments were conducted according to National Institutes of Health standards as set forth in the Guide for the Care and Use of Laboratory Animals, and were approved by the Committee on the Ethics of Animal

Experiments of the Hubei University of Science and Technology. To establish mouse tumor models, LLC cells (2.5×10^5 cells in 0.1 mL of PBS) were injected into the muscle at the right hind legs of male C57BL/6 mice. After the tumor volume reached a range between 50 and 200 mm^3, the hair of mice was removed using sodium sulfide solution (80 g/L in 30% ethanol). The mice (n=48) were randomly divided into 4 groups of 12 mice each. Mice in different groups were injected with DOX, CUR, DOX + CUR, or (DOX + CUR)–PMs via the tail vein; the equivalent DOX dose was 5 mg/kg, while the CUR dose was 1.6 times as much as DOX. Blood samples were collected using heparinized tubes (the starting time point was set as 5 s after injection) at different time intervals (0.08, 0.16, 0.5, 1, 2, 3, 6, 9, 12, 24, 48, and 72 h). Plasma samples were obtained by centrifugation at 4,000 rpm for 10 min, precipitated with methanol and analyzed using ultra-performance liquid chromatography–tandem mass spectrometry.

Antitumor efficacy

LLC tumor-bearing C57BL/6 mice (n=25) were randomly divided into 4 groups: 1) control group (normal saline), 2) DOX group, 3) DOX + CUR group, and 4) (DOX + CUR)–PMs group. Before injection, all mice were marked and weighed, and the length and width of tumors were measured to determine their initial volume. The day of injection was designated as Day 1. In Groups 2, 3, and 4, mice were injected with DOX, DOX + CUR, and (DOX + CUR)–PMs via the tail vein, respectively, and injection for each group was given on Day 1, Day 3, and Day 5. The equivalent DOX dose was 5 mg/kg, while the CUR dose was 1.6 times as much as DOX. With regard to the control group (Group 1), the mice were injected with the same volume of normal saline. The tumor size was measured every other day, and the tumor volume was estimated by the following formula:[32]

$$V\,(mm^3) = [\text{length} \times \text{width}^2]/2 \quad (3)$$

Statistical analysis

Data were expressed as mean ± standard deviation. Statistical analyses were carried out using statistical software (GraphPad Prism). One-way analysis of variance was used to examine whether significant differences existed between the measured data, and $P<0.05$ was considered to be statistically significant.

Results

Basic parameters of micelles

In this study, an attempt was made to develop a new type of drug-loaded micelle that can reverse MDR of certain lung cancer cells. Under optimal assembling conditions, some desirable (DOX + CUR)–PMs were obtained, and typical results are presented in Figure 2. The TEM image in Figure 2A shows that these micelles had sizes of ~20 nm and were without aggregation. Figure 2B shows that the size distribution of (DOX + CUR)–PMs had an approximate Gaussian distribution character, and the average size of the (DOX + CUR)–PMs calculated from Figure 2B is 17.02±2.58 nm (polydispersity index: 0.22). These (DOX + CUR)–PMs were also assessed for their zeta potential, and they were found to be nearly neutral with very small zeta potential of 0.37±0.014 mV. The DL of DOX and CUR in (DOX + CUR)–PMs was found to be 6.14% and 9.82%, respectively, and the matched LE was determined to be 81.8%±0.91% for DOX and 86.4%±0.36% for CUR. In addition, the critical aggregation concentration of (DOX + CUR)–PMs was estimated to be 0.04±0.0039 mg/mL. Based on these

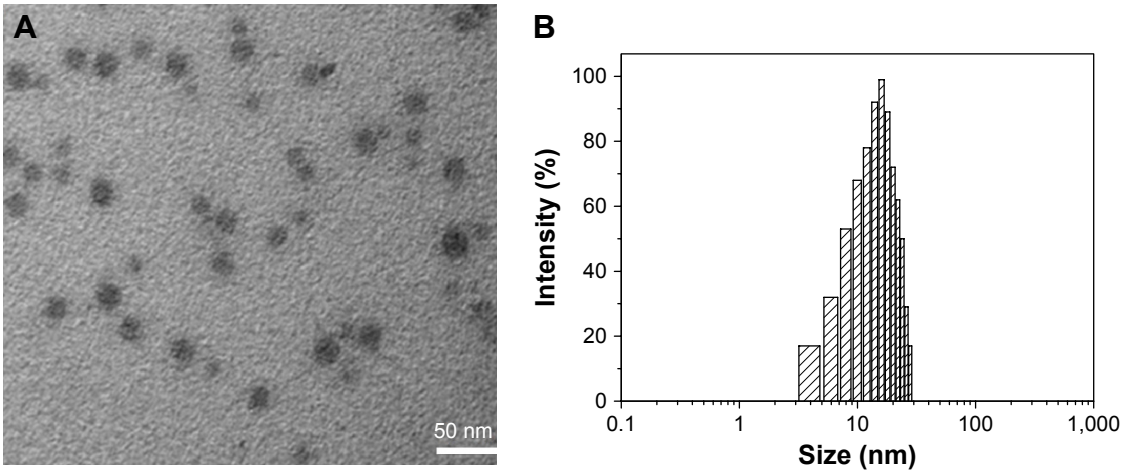

Figure 2 Physical characteristics of (DOX + CUR)–PMs.
Notes: (**A**) Representative TEM image and (**B**) size distribution of (DOX + CUR)–PMs.
Abbreviations: CUR, curcumin; DOX, doxorubicin; (DOX + CUR)–PMs, polymeric micelles loaded with DOX and CUR; TEM, transmission electron microscopy.

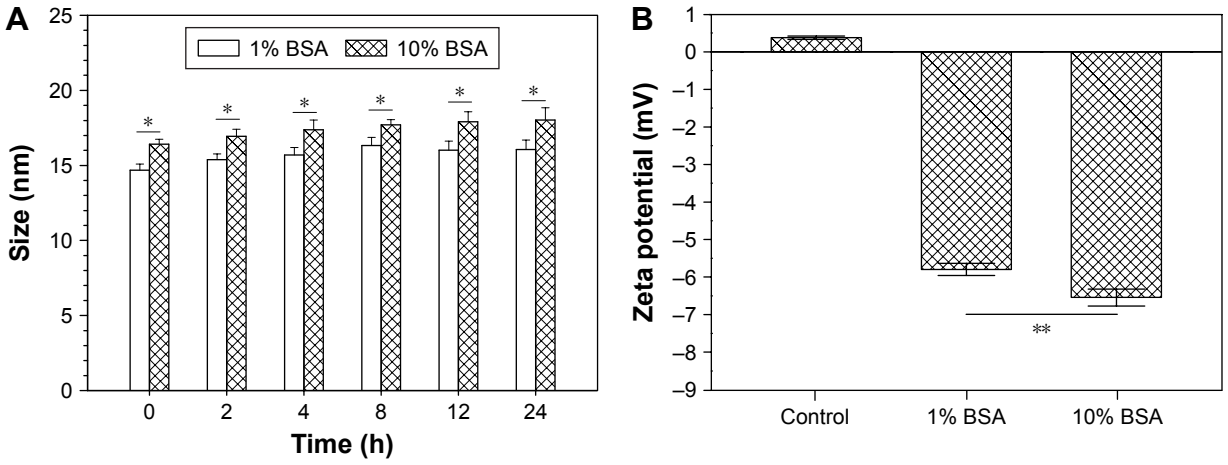

Figure 3 Colloidal stability of (DOX + CUR)–PMs in 1% and 10% BSA solutions.
Notes: (**A**) Size changes of (DOX + CUR)–PMs cultured in 1% and 10% BSA solutions at 37°C. (**B**) Changes in zeta potential of (DOX + CUR)–PMs cultured in 1% and 10% BSA solutions at 37°C for 24 h; n=3; *$P<0.05$; **$P<0.01$. The error bars represent standard deviation.
Abbreviations: CUR, curcumin; DOX, doxorubicin; (DOX + CUR)–PMs, polymeric micelles loaded with DOX and CUR; BSA, bovine serum albumin.

results, it can be concluded that these micelles have potential for practical applications due to their small sizes and clinically acceptable DLs.[2,3]

To examine the colloidal stability of (DOX + CUR)–PMs, they were dispersed in 1% and 10% aqueous BSA solutions to test whether any precipitation occurred; the size and zeta potential of the micelles were also measured, and the relevant data collected over 24 h are presented in Figure 3. There was no visualized precipitation of the micelles when they were exposed to these BSA solutions. Results in Figure 3A reveal that the BSA concentration had a significant impact ($P<0.05$) on the size of (DOX + CUR)–PMs and that higher BSA concentration resulted in larger sizes; moreover, at a fixed BSA concentration, the size of the micelles did not significantly change with increasing incubation time. Data in Figure 3B indicate that the zeta potential of (DOX + CUR)–PMs became negative when they were in 1% or 10% BSA aqueous solutions and that the BSA concentration significantly influenced the zeta potential of micelles. This can be ascribed to the coating effect of BSA on the micelles. It is known that the isoelectric point of BSA is about 4.7, and thus, BSA carries negative charges at neutral pH. As a result, BSA-coated (DOX + CUR)–PMs in solution should show negative zeta potential; and a concentrated BSA solution would cause stronger coating effect on the micelles, leading to more negative zeta potential. These results reveal that these micelles are stable in BSA aqueous solutions.

Release profiles of micelles

The release profiles of (DOX + CUR)–PMs are illustrated in Figure 4. It is observed that (DOX + CUR)–PMs released the loaded DOX at rapid rates in the first few hours, and the cumulative amount of released DOX reached about 50% within 4 h. Thereafter, their release rates became very slow. The pattern for CUR shows that (DOX + CUR)–PMs released CUR in a similar manner, but the release rate of CUR was significantly lower ($P<0.05$) than that of DOX until the release time reached about 6 h.

Cytotoxicity of micelles

L929 cells, a type of normal murine fibroblasts, were used to assess whether there is any cytotoxicity after they are treated with blank micelles, and the relevant results for the viability of L929 cells are presented in Figure 5. The cell viability was higher than 98% after 48 h incubation when the applied

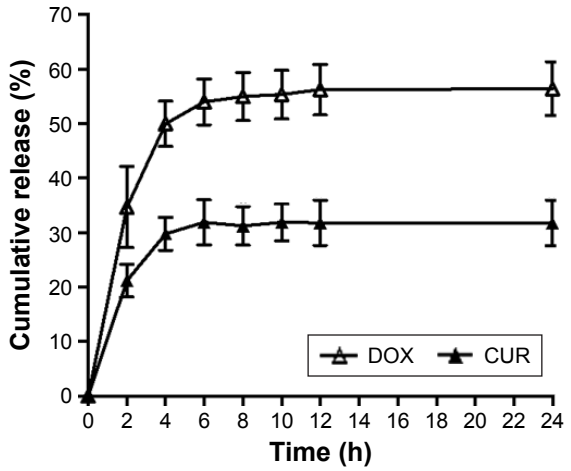

Figure 4 Cumulative release profiles of (DOX + CUR)–PMs.
Notes: n=3. The error bars represent standard deviation.
Abbreviations: CUR, curcumin; DOX, doxorubicin; (DOX + CUR)–PMs, polymeric micelles loaded with DOX and CUR.

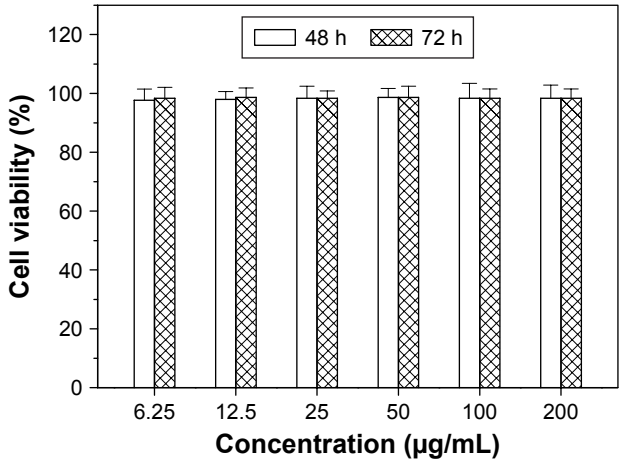

Figure 5 Viability of L929 cells treated with blank micelles at various micelle doses and cultured for different periods of time.
Note: n=3. The error bars represent standard deviation.

dose of the blank micelles changed from 6.25 to 200 μg/mL. After incubation for an extended period up to 72 h, a similar situation was observed. These results suggest that the blank micelles are nontoxic to normal cells.

The viability of A549 and A549/Adr cells exposed to varied amounts of DOX, DOX + CUR, and (DOX + CUR)–PMs is presented in Figure 6. Considering that A549 cells belong to the DOX-sensitive category of cells, the applied equivalent dose of DOX was selected as 1 μg/mL or less. In Figure 6A and B, DOX (concentration producing a 50% decrease of viability [IC_{50}]: 1.03 μg/mL, 48 h) and DOX + CUR (IC_{50}: 0.895 μg/mL, 48 h) showed similar cytotoxicity until the DOX concentration reached about 0.6 μg/mL, and after that, as the concentration further increased, DOX + CUR had higher cytotoxicity toward A549 cells than DOX alone. On the other hand, (DOX + CUR)–PMs (IC_{50}: 0.648 μg/mL, 48 h) displayed notably higher cytotoxicity than the other two, starting from a concentration of 0.4 μg/mL.

For the A549/Adr cells, the applied equivalent DOX dose was set in a range between 1 and 30 μg/mL due to the DOX-resistant properties of A549/Adr cells. As shown in Figure 6C and D, DOX + CUR (IC_{50}: 22.7 μg/mL, 48 h) had much higher cytotoxicity toward A549/Adr cells than DOX (IC_{50}: 37.9 μg/mL, 48 h) alone starting from a concentration

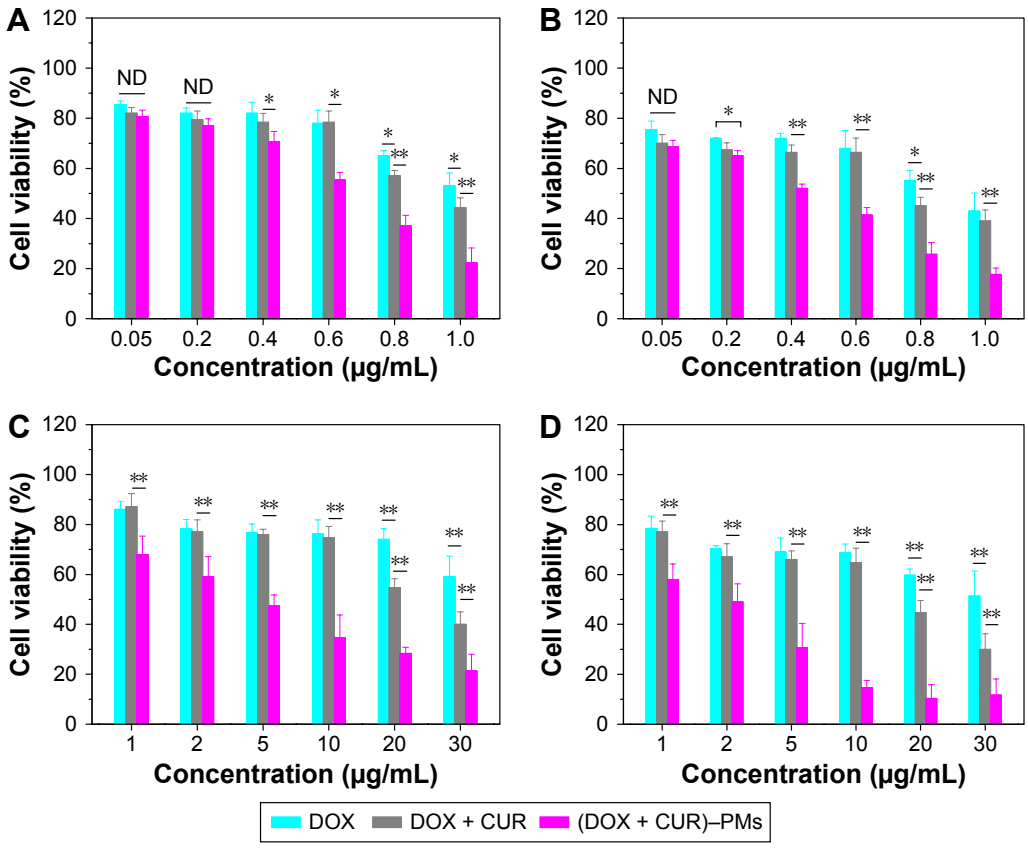

Figure 6 Cytotoxicity of various DOX formulations toward A549 cells and A549/Adr cells.
Notes: (**A**) A549 cells cultured for 48 h. (**B**) A549 cells cultured for 72 h. (**C**) A549/Adr cells cultured for 48 h. (**D**) A549/Adr cells cultured for 72 h. n=3; *$P<0.05$; **$P<0.01$. The error bars represent standard deviation.
Abbreviations: CUR, curcumin; DOX, doxorubicin; (DOX + CUR)–PMs, polymeric micelles loaded with DOX and CUR; ND, no difference.

of 20 μg/mL, and (DOX + CUR)–PMs (IC_{50}: 3.95 μg/mL, 48 h) exhibited considerably enhanced cytotoxicity than the other two starting from a concentration of 1 μg/mL.

Cellular uptake

To visualize the uptake into A549/Adr cells, the cells were incubated with DOX, CUR, DOX + CUR, and (DOX + CUR)–PMs for 2 h, and the uptake events were examined using CLSM. The images displayed in Figure 7A indicate that a very small amount of DOX was taken up by the cells. Figure 7B shows that CUR was more easily internalized by A549/Adr cells as compared to DOX. The red fluorescence with high brightness in Figure 7C confirms that the uptake of DOX was greatly enhanced when A549/Adr cells were treated with a combination of DOX and CUR. The images presented in Figure 7D exhibit that most of the CUR and DOX had already entered the nucleoli of A549/Adr cells when (DOX + CUR)–PMs were applied.

Uptake mechanism

A549/Adr cells without pretreatment using endocytosis inhibitors were incubated with (DOX + CUR)–PMs at the two different temperatures of 4°C and 37°C to see the difference in the uptake of (DOX + CUR)–PMs. Typical flow cytometric patterns for these two cases are presented in Figure 8A. It can be observed that there was a large difference in the endocytosis of (DOX + CUR)–PMs when the incubation temperature was set at 37°C and 4°C

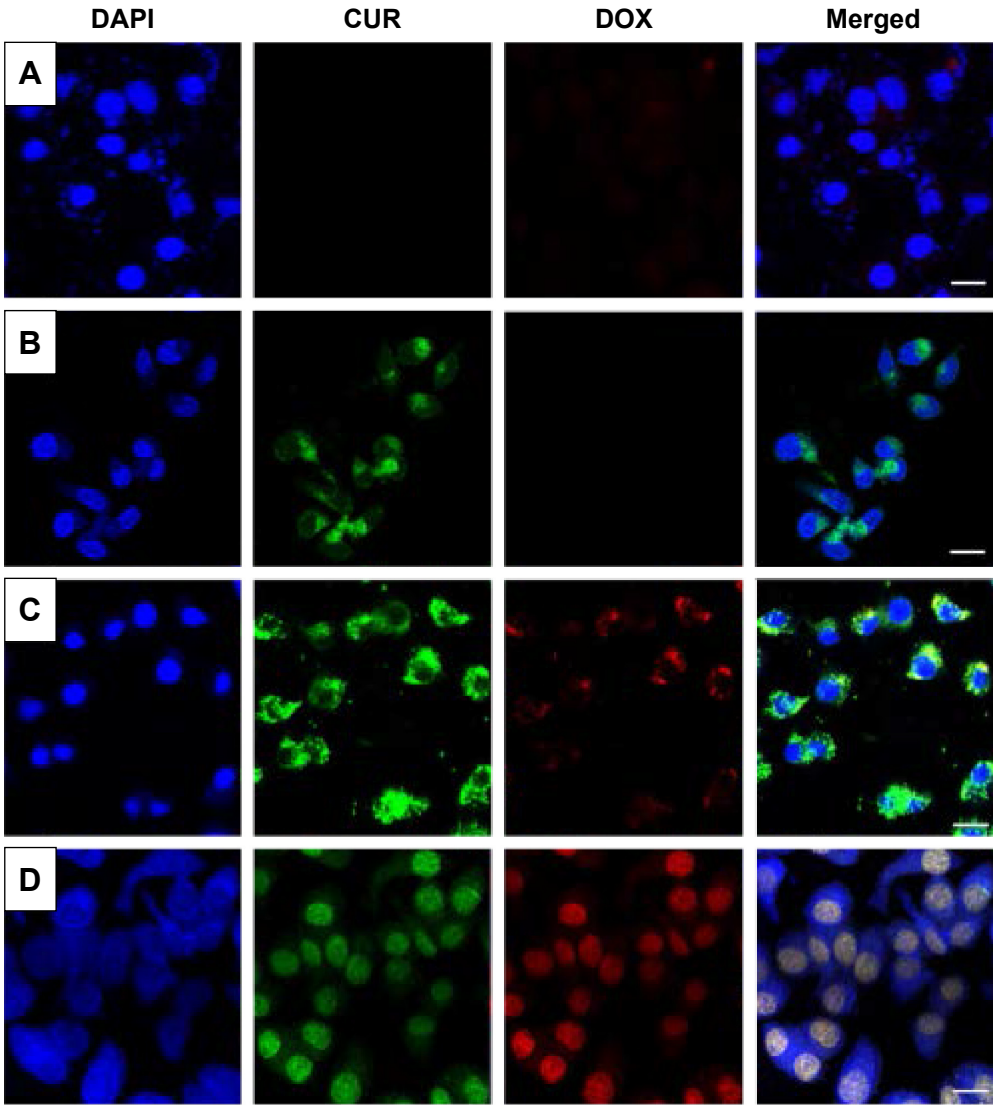

Figure 7 CLSM images for A549/Adr cells after 2 h incubation.
Notes: (**A**) DOX. (**B**) CUR. (**C**) DOX + CUR. (**D**) (DOX + CUR)–PMs (scale bar: 40 μm; blue color: DAPI nucleus staining, λ_{em} =488 nm, λ_{ex} =364 nm; red color: DOX, λ_{em} =593 nm, λ_{ex} =469 nm; green color: CUR, λ_{em} =475 nm, λ_{ex} =442 nm).
Abbreviations: CLSM, confocal laser scanning microscopy; CUR, curcumin; DAPI, 4′,6-diamidino-2-phenylindole; DOX, doxorubicin; (DOX + CUR)–PM, polymeric micelles loaded with DOX and CUR.

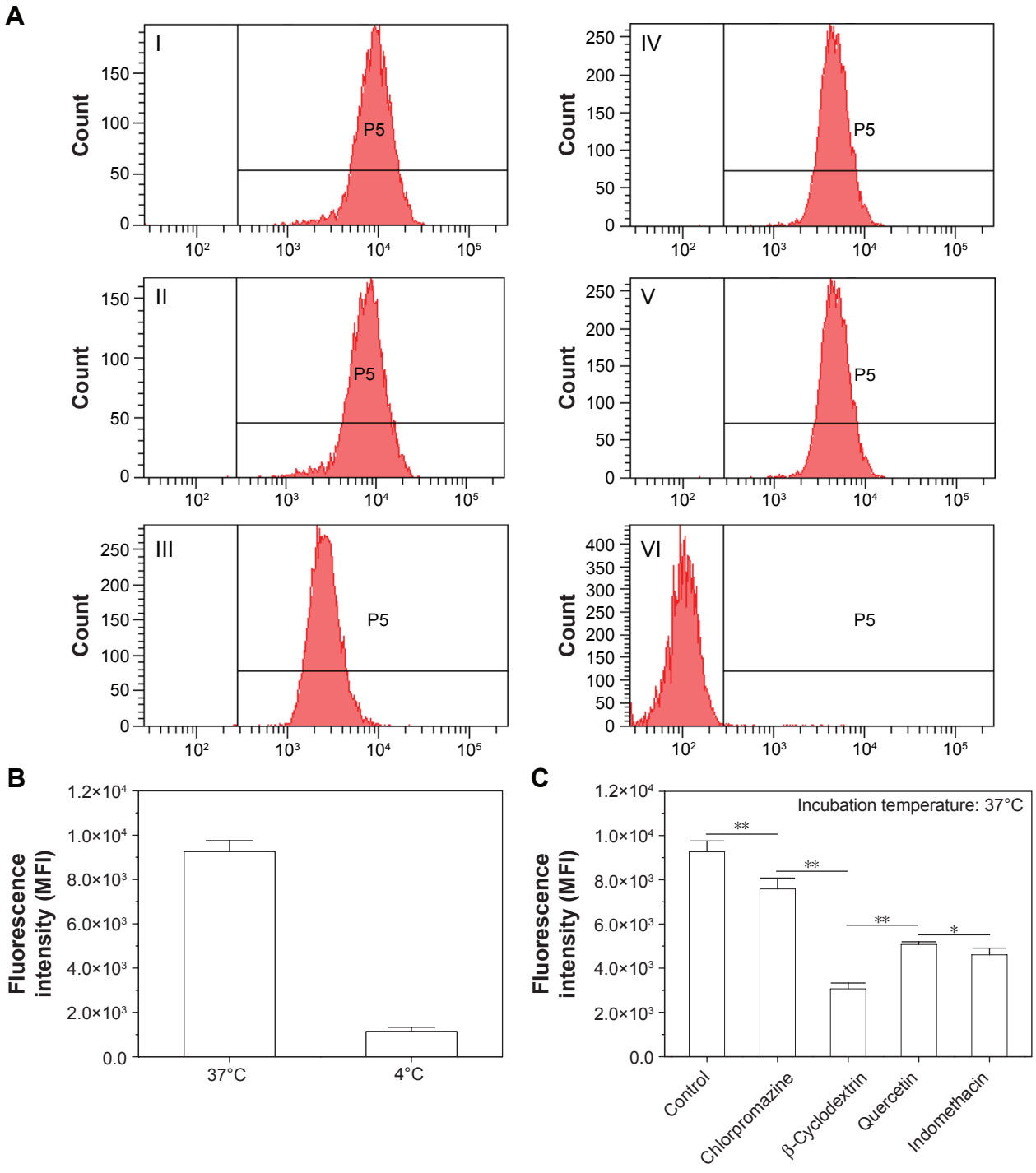

Figure 8 Flow cytometric measurements for endocytosis of (DOX + CUR)–PMs in A549/Adr cells with or without pretreatment with different endocytosis inhibitors.
Notes: (**A**) 37°C, I: control, no pretreatment with endocytosis inhibitors; II: 37°C, chlorpromazine; III: 37°C, β-cyclodextrin; IV: 37°C, quercetin; V: 37°C, indomethacin; and VI: 4°C, no pretreatment with endocytosis inhibitors. (**B**) Average fluorescence intensity at different temperatures. (**C**) Average fluorescence intensity at a fixed temperature of 37°C; n=3; *$P<0.05$; **$P<0.01$. The error bars represent standard deviation. "P5" is the "gate number" that was set automatically by the instrument, and it means that data shown in this gate are positive.
Abbreviations: DOX, doxorubicin; CUR, curcumin; (DOX + CUR)–PMs, polymeric micelles loaded with DOX and CUR.

(I and VI, respectively, in Figure 8A for these two cases). More samples cultured respectively at 4°C and 37°C were measured, and the average fluorescence intensity is depicted in Figure 8B. The bar graphs in Figure 8B show that the endocytosis of (DOX + CUR)–PMs at 37°C was around 8-fold higher than that measured at 4°C, verifying that the endocytosis pathway of (DOX + CUR)–PMs in A549/Adr cells was highly energy dependent. To facilitate the endocytosis of (DOX + CUR)–PMs, all follow-up incubations were conducted at 37°C.

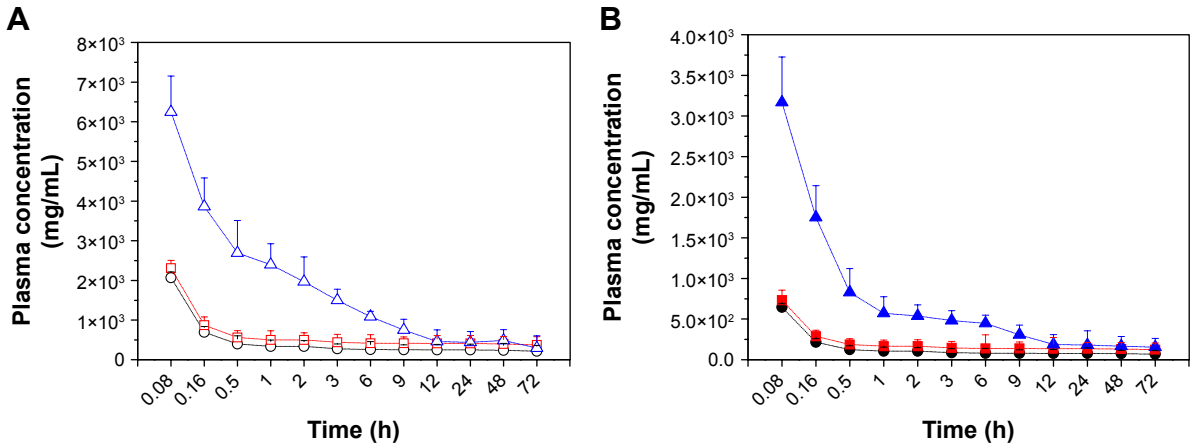

Figure 9 Time-dependent plasma concentrations of DOX and CUR in mice after administration of different agents.
Notes: DOX dose: 5 mg/kg; and CUR dose: 8 mg/kg. (**A**) Plasma concentrations of DOX. Open triangle: (DOX + CUR)–PMs; open square: DOX + CUR; and open circle: free DOX. (**B**) Plasma concentrations of CUR. Solid triangle: (DOX + CUR)–PMs; solid square: DOX + CUR; solid circle: free CUR (n=5). The error bars represent standard deviation.
Abbreviations: DOX, doxorubicin; CUR, curcumin; (DOX + CUR)–PMs, polymeric micelles loaded with DOX and CUR.

A549/Adr cells pretreated with the four types of endocytosis inhibitors were incubated with (DOX + CUR)–PMs at 37°C to find out the possible uptake mechanism, and the relevant flow cytometric patterns for these cases are also represented in Figure 8A (II, III, IV, and V, respectively, for these four cases). To quantitatively compare the effects of endocytosis inhibitors on the uptake of (DOX + CUR)–PMs, more samples corresponding to each kind of inhibitor were measured, and their average fluorescence intensity is illustrated in Figure 8C.

In vivo clearance

After intravenous administration of DOX, CUR, DOX + CUR, and (DOX + CUR)–PMs for predetermined time intervals, time-dependent concentrations of DOX and CUR in plasma of mice were measured, and the relevant results are presented in Figure 9. As shown in Figure 9A, the plasma concentration of DOX (open circles) quickly dropped down to a very low level within 0.5 h when free DOX was applied; injection of DOX + CUR (open squares) did not result in any significant difference in the plasma concentrations of DOX when compared to the injection of DOX alone; and in the case of (DOX + CUR)–PMs, the plasma concentrations of DOX were notably higher ($P<0.01$) than those measured in the two other cases over a period of 6 h of in vivo circulation. Similar observations for the plasma concentrations of CUR were registered in Figure 9B. Injection of free CUR or a DOX + CUR combination did not significantly influence the plasma concentrations of CUR, and in the case of (DOX + CUR)–PMs, the plasma concentration of CUR during a 6 h circulation period was significantly higher ($P<0.01$) than that detected in the two other cases.

In vivo antitumor efficacy

Antitumor effects of different DOX formulations were evaluated using LLC tumor-bearing C57BL/6 mice. The variation of tumor volume with time is shown in Figure 10A. It was observed that the tumor volume of mice in the control group increased starting from Day 5; after injection of DOX alone or in combination with CUR, the tumor volume of mice significantly reduced when compared to that in the control group, and a combination of DOX and CUR showed significantly higher efficiency against the growth of tumor. To see the differences in tumor volumes more clearly, two curves for the free DOX + CUR combination and for the (DOX + CUR)–PMs in Figure 10A are expanded and displayed in Figure 10B. The changes in body weight of mice were also monitored, and the relevant data are depicted in Figure 10C.

Discussion

In principle, starting materials for assembling micelles are important because they are closely correlated to the size and surface properties of the resulting micelles, as well as their loading capacity. In this study, DSPE-PEG_{2000} was selected as a starting material considering that it is an amphiphilic copolymer and can be self-assembled into uniform micelles with small sizes.[27] Another starting material, $TPGS_{1000}$, was used together with DSPE-PEG_{2000} to endue the resulting micelles with a new ability to inhibit the functions of P-gp and, in turn, to overcome the MDR of certain cancer cells.

Based on preliminary trials, it was found that micelles could be assembled using a regular film-forming technique, and the DSPE-PEG_{2000} component in micelles had a high tolerance for the coexistence of the $TPGS_{1000}$ component.

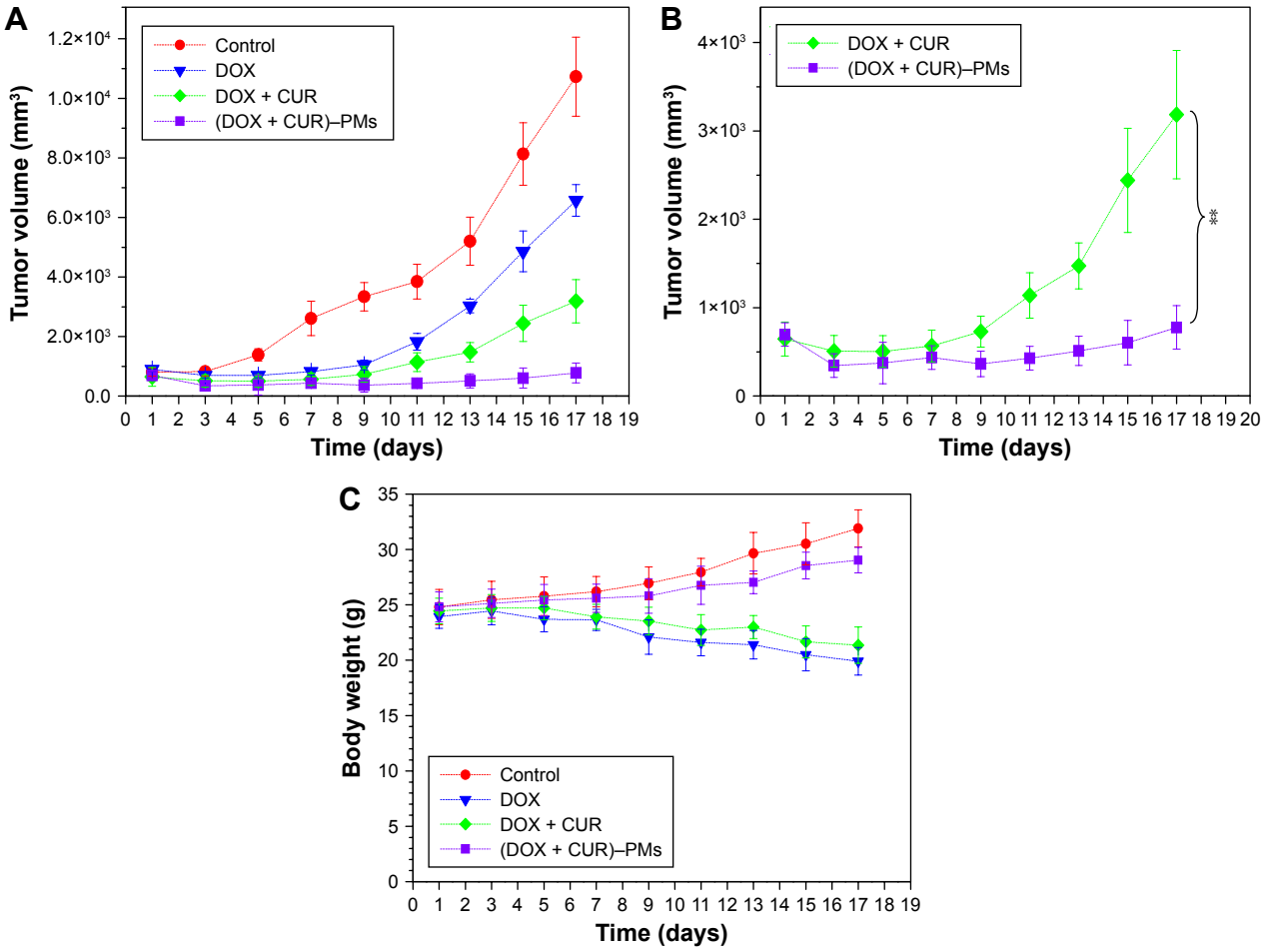

Figure 10 Variations in tumor size with time after administration of different agents and changes in body weight of mice.
Notes: (**A**) Variations in tumor size with time after administration of DOX, DOX + CUR, and (DOX + CUR)–PMs. (**B**) Two expanded curves quoted from (**A**). (**C**) Changes in body weight of LLC tumor-bearing mice treated with different agents; n=5; $^{**}P<0.01$. The error bars represent standard deviation.
Abbreviations: DOX, doxorubicin; CUR, curcumin; (DOX + CUR)–PM, polymeric micelles loaded with DOX and CUR; LLC, Lewis lung carcinoma.

Although several processing parameters could affect the micelle assembly, the ratio of $TPGS_{1000}$ to $DSPE\text{-}PEG_{2000}$ and their concentration in the blend solutions were found to act as the main factors for controlling the size and LE of micelles. These two parameters were thus optimized to prepare small-sized micelles. The results shown in Figure 2 confirm that the materials used and the applied assembly technique are suitable for achieving small-sized micelles. The small size of (DOX + CUR)–PMs is propitious to target tumors through the enhanced permeability and retention (EPR) effect.[22,23] On the other hand, these (DOX + CUR)–PMs have just the right sizes that allow them to avoid clearance either by renal infiltration (<10 nm) or by the reticuloendothelial system (RES) (>100 nm).[33]

Figure 4 indicates that the two release curves are composed of a rapid ascent section and a following plateau region, and there are significant differences in the release rates between them until the release time reaches around 6 h. As described in the "Assembly of PMs" section, both DOX and CUR were incorporated into micelles by physical and hydrophobic interactions during the assembly of micelles, and thus, DOX and CUR would easily diffuse through pores or channels existing on the surfaces of micelles when the micelles are exposed to the release medium, leading to the fast release of DOX and CUR at the early stage. After being released for a period of time, the core of micelles could become compact due to the reduction of entrapped drugs, resulting in the subsequent slow release. With regard to the relatively slow release rate for CUR, the possible reason is that CUR has relatively strong hydrophobicity than DOX.

It is known that CUR is able to sensitize many types of cancer cells and to inhibit them from proliferating.[15,16] In comparison to free DOX, the enhanced cytotoxicity for A549 cells arising from DOX + CUR at higher doses can be attributed to the synergistic effects of DOX and CUR (Figure 6A and B). As mentioned in the "Assembly of PMs" section, DOX had

been desalted to facilitate its loading, and hence, deprotonated DOX became somewhat hydrophobic. On the other hand, CUR is known to be hydrophobic, and in particular, it can be easily degraded under physiological conditions.[19,34] In contrast to free CUR, the loaded CUR in (DOX + CUR)–PMs would be completely protected from degradation before CUR gets into cells, and thus, more CUR molecules with sensitizing activity can finally be transferred into the cells during the endocytosis of (DOX + CUR)–PMs compared to the case of the simple combination of DOX and CUR. As a result, (DOX + CUR)–PMs result in enhanced cytotoxicity toward A549 cells, as shown in Figure 6.

It is well established that P-gp has a membrane pump function associated with ATP, and it is able to pump out the internalized drugs, leading to the occurrence of MDR of cancer cells.[35] By comparing Figure 6A with Figure 6C, it can be seen that the viability of A549 cells treated with free DOX at a dose of 1 μg/mL is similar to that of A549/Adr cells exposed to free DOX at a dose of 30 μg/mL. The poor ability of free DOX to inhibit the growth A549/Adr cells can be ascribed to the overexpression of P-gp in A549/Adr cells.

It has been reported that CUR has the ability to suppress the pumping function of P-gp expressed in malignancies involving lung, colon, and other tissues.[36,37] Therefore, in contrast to DOX alone, the stronger inhibitory effect of DOX + CUR on the growth of A549/Adr cells can be attributed to the synergistic actions of DOX + CUR. In the case of (DOX + CUR)–PMs, the component $TPGS_{1000}$ present in the micelles has inhibiting functions against P-gp,[27,31] and on the other hand, micelles could help to transfer more CUR molecules into A549/Adr due to the protection functions of micelles. Therefore, the actions of DOX, CUR, and $TPGS_{1000}$ synergistically enable (DOX + CUR)–PMs to have much higher cytotoxicity toward A549/Adr cells in comparison to the simple combination of DOX and CUR.

The very low internalized amount of DOX presented in Figure 7A can be ascribed to the DOX-resistant properties of A549/Adr cells. In comparison to the case illustrated in Figure 7A, the internalization of CUR shown in Figure 7B is notably enhanced, confirming that CUR has certain ability to avoid exocytosis by A549/Adr cells. The merged image displayed in Figure 7C reveals that most of the internalized CUR and DOX resided in the cytoplasm of A549/Adr cells instead of nucleoli, suggesting that the DOX-resistant properties of A549/Adr cells have been partially overcome in the presence of CUR because the internalized DOX was still observed inside cells after 2 h incubation. The images shown in Figure 7D demonstrate that $TPGS_{1000}$/DSPE-PEG_{2000}-assembled micelles can function as effective carriers for delivering both DOX and CUR into A549/Adr cells by reversing the MDR of A549/Adr cells because most of the CUR and DOX moieties had already entered the nucleoli of A549/Adr cells.

Figure 7C indicates that a small amount of free CUR already enters the nucleoli of A549/Adr cells, but most of the free DOX is located in the cytoplasm. This can be ascribed to the property of A549/Adr cells. It is known that A549/Adr cells belong to the category of DOX-resistant cells, and thus, the internalized free DOX could be eliminated via the MDR pathway before they can reach the nucleoli of A549/Adr cells. Concomitantly, the internalized free CUR could also face degradation because of the enzyme-containing microenvironment inside the cells. In the case of (DOX + CUR)–PMs, DOX and CUR are internalized into A549/Adr cells via micelle carriers, and hence, DOX and CUR are able to stay inside the cytoplasm for a much longer time than free DOX and free CUR due to the protection of micelle carriers, allowing them to have high opportunity to enter the nucleoli of A549/Adr cells.

To find out the possible mechanism for the uptake of (DOX + CUR)–PMs into A549/Adr cells, the cells were exposed to (DOX + CUR)–PMs together with one of the designated pathway inhibitors. In this study, several pathway inhibitors, namely, chlorpromazine, β-cyclodextrin, quercetin, and indomethacin, were selected considering that the endocytosis mechanisms of these inhibitors have been clearly elucidated.[38–41] Chlorpromazine is reported to be a clathrin-dependent endocytosis inhibitor, and the inhibiting effect of β-cyclodextrin is mediated by caveolae/lipid raft.[38] Quercetin has clathrin- and caveolin-dependent characteristics,[39,40] and the inhibiting function of indomethacin is related to caveolin mediation.[41]

In Figure 8, it can be observed that in comparison to the control (without pretreatment using endocytosis inhibitor), chlorpromazine has a limited impact on the internalization of (DOX + CUR)–PMs; β-cyclodextrin greatly inhibits the uptake of (DOX + CUR)–PMs, while indomethacin and quercetin are also able to significantly inhibit the endocytosis of (DOX + CUR)–PMs. On this basis, it can be inferred that the cellular uptake of (DOX + CUR)–PMs in A549/Adr cells is controlled via a multifactorial mechanism that is associated with energy-dependent, caveolae-mediated, and clathrin-independent endocytosis.

Results illuminated in Figure 9 reveal that a simple combination of DOX and CUR will not help to increase the

plasma concentration of DOX or CUR, and that the co-delivery of DOX and CUR via herein-designed micelles is effective for significantly increasing the blood concentration of DOX or CUR and prolonging their respective blood circulation time. The reason for the prolonged circulation of (DOX + CUR)–PMs and the matching high plasma concentration of DOX or CUR can be ascribed to the properties of micelles. As mentioned earlier, (DOX + CUR)–PMs had an average size of around 17 nm, which allows micelles to avoid the clearance by rental infiltration or by RES.[31] On the other hand, (DOX + CUR)–PMs had hydrophilic surface due to the presence of PEG segments, which would help micelles to evade the opsonization of various proteins in blood and the cytophagy related to mononuclear macrophages.[42,43]

Data shown in Figure 10 demonstrate that the growth of tumor in the group treated with (DOX + CUR)–PMs is notably inhibited as compared to that treated either with DOX alone or with the combination of DOX and CUR. The high efficiency of (DOX + CUR)–PMs in inhibiting the growth of tumors can be attributed to the long circulation time and the EPR effects of the micelles themselves as well as the synergistic actions of DOX, CUR and $TPGS_{1000}$ against the tumors.

Body weight of mice in the control group gradually increased with time, and it is attributed to the regular growth of tumor-bearing mice. The body weight of mice in the groups treated with free DOX or a DOX + CUR combination shows a weight-reducing tendency starting from around 1 wk after the first injection, revealing that toxic effects are produced by DOX or the mixture of DOX and CUR. The body weight of mice in the groups treated with (DOX + CUR)–PMs increases at relatively low rates as compared to the control group, which could be attributed to the reduced side effects of the loaded drugs due to the drug's encapsulation inside micelles.[24]

Conclusion

PMs loaded with DOX and CUR were successfully assembled using $TPGS_{1000}$ and DSPE-PEG_{2000} as component materials, and their size, DL, and LE could be regulated by the ratio of $TPGS_{1000}$ to DSPE-PEG_{2000} and by the concentration of the mixed solutions. Under optimal assembly conditions, the resultant micelles showed definite ability to deliver both DOX and CUR into DOX-resistant A549/Adr cells and, meanwhile, to synergistically reverse the DOX resistance of A549/Adr cells. In vivo examinations confirmed that the micelles had capability to increase the plasma concentration of DOX or CUR and to prolong their respective circulation in blood stream. In addition, these micelles were able to significantly inhibit tumor growth in LLC tumor-bearing mice. These results suggest that the herein-developed micelles have potential in the treatment of lung cancer.

Acknowledgments

This work was supported by the Wu Jieping Medical Foundation of China (grant number 320675013228), the Research Foundation of Hubei University of Science and Technology (grant number BK1432), and the National Natural Science Foundation of China (grant number 81371705).

Disclosure

The authors report no conflicts of interest in this work.

References

1. Gottesman MM. Mechanisms of cancer drug resistance. *Annu Rev Med*. 2002;53:615–627.
2. Hurley LH. DNA and its associated processes as targets for cancer therapy. *Nat Rev Cancer*. 2002;2(3):188–200.
3. Gottesman MM, Fojo T, Bates SE. Multidrug resistance in cancer: role of ATP-dependent transporters. *Nat Rev Cancer*. 2002;2(1):48–58.
4. Ding J, Xiao C, Li Y, et al. Efficacious hepatoma-targeted nanomedicine self-assembled from galactopeptide and doxorubicin driven by two-stage physical interactions. *J Control Release*. 2013;169(3):193–203.
5. Chen J, Ding J, Zhang Y, Xiao C, Zhuang X, Chen X. Polyion complex micelles with gradient pH-sensitivity for adjustable intracellular drug delivery. *Polym Chem*. 2015;6(3):397–405.
6. Ding J, Chen J, Li D, et al. Biocompatible reduction-responsive polypeptide micelles as nanocarriers for enhanced chemotherapy efficacy *in vitro*. *J Mater Chem B*. 2013;1(1):69–81.
7. Li D, Ding JX, Tang ZH, et al. *In vitro* evaluation of anticancer nanomedicines based on doxorubicin and amphiphilic Y-shaped copolymers. *Int J Nanomedicine*. 2012;7:2687–2697.
8. Lien C, Jensen B, Hydock D, Hayward R. Short-term exercise training attenuates acute doxorubicin cardiotoxicity. *J Physiol Biochem*. 2015;71(4):669–678.
9. Chen Y, Zhang W, Huang Y, Gao F, Sha X, Fang X. Pluronic-based functional polymeric mixed micelles for co-delivery of doxorubicin and paclitaxel to multidrug resistant tumor. *Int J Pharm*. 2015;488(1–2):44–58.
10. Pramanik D, Campbell NR, Das S, et al. A composite polymer nanoparticle overcomes multidrug resistance and ameliorates doxorubicin-associated cardiomyopathy. *Oncotarget*. 2012;3(6):640–650.
11. Mittal A, Tabasum S, Singh R. Berberine in combination with doxorubicin suppresses growth of murine melanoma B16F10 cells in culture and xenograft. *Phytomedicine*. 2014;21(3):340–347.
12. Tong N, Zhang J, Chen Y, et al. Berberine sensitizes multiple human cancer cells to the anticancer effects of doxorubicin *in vitro*. *Oncol Lett*. 2012;3(6):1263–1267.
13. Al-Abd A, Mahmoud A, El-Sherbiny G, et al. Resveratrol enhances the cytotoxic profile of docetaxel and doxorubicin in solid tumour cell lines *in vitro*. *Cell Prolif*. 2011;44(6):591–601.
14. Osman A, Bayoumi H, Al-Harthi S, Damanhouri Z, Elshal M. Modulation of doxorubicin cytotoxicity by resveratrol in a human breast cancer cell line. *Cancer Cell Int*. 2012;12(1):47–54.
15. Aggarwal BB, Sung B. Pharmacological basis for the role of curcumin in chronic diseases: an age-old spice with modern targets. *Trends Pharmacol Sci*. 2009;30(2):85–94.
16. Meiyanto E, Putri DD, Susidarti RA, et al. Curcumin and its analogues (PGV-0 and PGV-1) enhance sensitivity of resistant MCF-7 cells to doxorubicin through inhibition of HER2 and NF-κB activation. *Asian Pac J Cancer Prev*. 2014;15(1):179–184.

17. Choi BH, Kim CG, Lim Y, Shin SY, Lee YH. Curcumin down-regulates the multidrug-resistance mdr1b gene by inhibiting the PI3K/Akt/NF kappa B pathway. *Cancer Lett*. 2008;259(1):111–118.
18. Shukla S, Zaher H, Hartz A, Bauer B, Ware JA, Ambudkar SV. Curcumin inhibits the activity of ABCG2/BCRP1, a multidrug resistance-linked ABC drug transporter in mice. *Pharm Res*. 2009;26(2):480–487.
19. Zhou N, Zan X, Wang Z, et al. Galactosylated chitosan-polycaprolactone nanoparticles for hepatocyte-targeted delivery of curcumin. *Carbohydr Polym*. 2013;94(1):420–429.
20. Das RK, Kasoju N, Bora U. Encapsulation of curcumin in alginate-chitosan-pluronic composite nanoparticles for delivery to cancer cells. *Nanomed Nanotechnol Biol Med*. 2010;6:153–160.
21. Duan J, Mansour HM, Zhang Y, et al. Reversion of multidrug resistance by co-encapsulation of doxorubicin and curcumin in chitosan/poly(butyl cyanoacrylate) nanoparticles. *Int J Pharm*. 2012;426(1–2):193–201.
22. Wang BL, Shen YM, Zhang QW, et al. Codelivery of curcumin and doxorubicin by MPEG-PCL results in improved efficacy of systemically administered chemotherapy in mice with lung cancer. *Int J Nanomedicine*. 2013;8:3521–3531.
23. Barui S, Saha S, Mondal G, Haseena S, Chaudhuri A. Simultaneous delivery of doxorubicin and curcumin encapsulated in liposomes of pegylated RGDK-lipopeptide to tumor vasculature. *Biomaterials*. 2014; 35(5):1643–1656.
24. Zhao X, Chen Q, Liu W, et al. Codelivery of doxorubicin and curcumin with lipid nanoparticles results in improved efficacy of chemotherapy in liver cancer. *Int J Nanomedicine*. 2015;10:257–270.
25. Cesur H, Rubinstein I, Pai A, Onyuksel H. Self-associated indisulam in phospholipid-based nanomicelles: a potential nanomedicine for cancer. *Nanomedicine*. 2009;5(2):178–183.
26. Li X, Li P, Zhang Y, et al. Novel mixed polymeric micelles for enhancing delivery of anticancer drug and overcoming multidrug resistance in tumor cell lines simultaneously. *Pharm Res*. 2010;27(8):1498–1511.
27. Liu Y, Xu Y, Wu M, et al. Vitamin E succinate-conjugated F68 micelles for mitoxantrone delivery in enhancing anticancer activity. *Int J Nanomedicine*. 2016;11:3167–3178.
28. Collnot EM, Baldes C, Wempe MF, et al. Influence of vitamin E TPGS poly(ethylene glycol) chain length on apical efflux transporters in Caco-2 cell monolayers. *J Control Release*. 2006;111(1–2):35–40.
29. Shen R, Kim JJ, Yao M, Elbayoumi TA. Development and evaluation of vitamin E d-α-tocopheryl polyethylene glycol 1000 succinate-mixed polymeric phospholipid micelles of berberine as an anticancer nanopharmaceutical. *Int J Nanomedicine*. 2016;11:1687–1700.
30. Ma P, Dong XW, Swadley CL, et al. Development of idarubicin and doxorubicin solid lipid nanoparticles to overcome Pgp-mediated multiple drug resistance in leukemia. *J Biomed Nanotechnol*. 2009;5(2): 151–161.
31. Day CP, Carter J, Bonomi C, Hollingshead M, Merlino G. Preclinical therapeutic response of residual metastatic disease is distinct from its primary tumor of origin. *Int J Cancer*. 2012;130(1):190–199.
32. Unezaki S, Maruyama K, Hosoda JI, et al. Direct measurement of the extravasation of polyethyleneglycol-coated liposomes into solid tumor tissue by *in vivo* fluorescence microscopy. *Int J Pharm*. 1996; 144(1):11–17.
33. Wang J, Sun J, Chen Q, et al. Star-shape copolymer of lysine-linked ditocopherol polyethylene glycol 2000 succinate for doxorubicin delivery with reversal of multidrug resistance. *Biomaterials*. 2012;33(28): 6877–6888.
34. Anand P, Kunnumakkara AB, Newman RA, Aggarwal BB. Bioavailability of curcumin: problems and promises. *Mol Pharm*. 2007;4(6): 807–818.
35. Garcia-Gomes A, Curvelo J, Soares R, Ferreira-Pereira A. Curcumin acts synergistically with fluconazole to sensitize a clinical isolate of Candida albicans showing a MDR phenotype. *Med Mycol*. 2012;50(1):26–32.
36. Revalde J, Li Y, Hawkins B, Rosengren R, Paxton J. Heterocyclic cyclohexanone monocarbonyl analogs of curcumin can inhibit the activity of ATP-binding cassette transporters in cancer multidrug resistance. *Biochem Pharmacol*. 2015;93(3):305–317.
37. Si M, Zhao J, Li X, Tian JG, Li YG, Li JM. Reversion effects of curcumin on multidrug resistance of MNNG/HOS human osteosarcoma cells *in vitro* and *in vivo* through regulation of P-glycoprotein. *Chin Med J*. 2013;126(21):4116–4123.
38. Huang H, Feng X, Zhuang J, et al. Internalization of UT-A1 urea transporter is dynamin dependent and mediated by both caveolae- and clathrin-coated pit pathways. *Am J Physiol Renal Physiol*. 2010;299(6): F1389–F1395.
39. Volonte D, Zhang K, Lisanti M, Galbiati F. Expression of caveolin-1 induces premature cellular senescence in primary cultures of murine fibroblasts. *Mol Biol Cell*. 2002;13(7):2502–2517.
40. Sreeja S, Thampan R. Estradiol-mediated internalisation of the non-activated estrogen receptor from the goat uterine plasma membrane: identification of the proteins involved. *Mol Cell Biochem*. 2004; 259(1–2):131–140.
41. Irannejad H, Unsal Tan O, Ozadali K, et al. 1,2-Diaryl-2-hydroxyiminoethanones as dual COX-1 and β-amyloid aggregation inhibitors: biological evaluation and in silico study. *Chem Biol Drug Des*. 2015; 85(4):494–503.
42. Li J, Wu N, Wu J, Wan Y, Liu C. Effect of protein adsorption on cell uptake and blood clearance of methoxy poly(ethylene glycol)-poly (caprolactone) nanoparticles. *J Appl Polym Sci*. 2015;133(3):42884.
43. Yadav KS, Jacob S, Sachdeva G, Chuttani K, Mishra AK, Sawant KK. Long circulating PEGylated PLGA nanoparticles of cytarabine for targeting leukemia. *J Microencapsul*. 2011;28(8):729–742.